

fellowship for R. S. We thank Drs. R. Kirchner, R. G. Little, and A. P. Gaughan, Jr., for helpful discussions. This work was supported in part by the National Science Foundation.

Registry No. [Rh(CO)[P(C<sub>6</sub>H<sub>5</sub>)<sub>3</sub>]<sub>2</sub>](HCBP), 42063-67-2.

Supplementary Material Available. A listing of structure amplitudes and Table III, the root-mean-square amplitudes of vibration,

will appear following these pages in the microfilm edition of this volume of the journal. Photocopies of the supplementary material from this paper only or microfiche (105 × 148 mm, 24× reduction, negatives) containing all of the supplementary material for the papers in this issue may be obtained from the Journals Department, American Chemical Society, 1155 16th St., N.W., Washington, D. C. 20036. Remit check or money order for \$7.00 for photocopy or \$2.00 for microfiche, referring to code number INORG-74-2870.

Contribution from the Department of Chemistry and Institute of Materials Science, University of Connecticut, Storrs, Connecticut 06268

## Crystal Structure of Ferrous Phosphate, Fe<sub>3</sub>(PO<sub>4</sub>)<sub>2</sub>

E. KOSTINER\* and J. R. REA

Received July 1, 1974

AIC40429D

The crystal structure of ferrous phosphate has been determined and refined by full-matrix least-squares procedures using automatic diffractometer data to a residual  $R = 0.048$  ( $R_w = 0.066$ ) with a data:parameter ratio of 15. The space group is  $P2_1/c$  with  $a = 8.881$  (2) Å,  $b = 11.169$  (2) Å,  $c = 6.145$  (1) Å, and  $\beta = 99.36$  (3)°. Fe<sub>3</sub>(PO<sub>4</sub>)<sub>2</sub> is a pure end member of the series represented by the mineral graftonite—(Fe,Mn,Ca,Mg)<sub>3</sub>(PO<sub>4</sub>)<sub>2</sub>—and is isotypic with it. Ferrous ions occupy three distinct coordination polyhedra; the variations in cation coordination among the compounds crystallizing in this structure type are discussed.

### Introduction

The mineral graftonite, formulated as (Fe,Mn,Ca,Mg)<sub>3</sub>(PO<sub>4</sub>)<sub>2</sub>,<sup>1</sup> crystallizes in the space group  $P2_1/c$ .<sup>2</sup> Several compounds which are isotypic with graftonite have been reported in recent years differing slightly in the coordination polyhedra surrounding the three crystallographically unique cation sites. Table I lists each of these compounds along with their unit cell parameters and cation coordination numbers. We have prepared single crystals of an end member of the graftonite solid solution series—ferrous phosphate—and wish to present the results of our crystal structure refinement.

### Experimental Section

**Preparation and Crystal Growth.** Ferric phosphate, FePO<sub>4</sub>, was synthesized by the thermal decomposition and reaction of a stoichiometric mixture of reagent grade ferric oxide and ammonium dihydrogen phosphate at 1000° in air. Then, in a sealed evacuated quartz tube, a stoichiometric mixture of ferric phosphate and iron metal was heated at 800° for 24 hr (the heat treatment repeated twice after re-grinding) to produce ferrous phosphate.<sup>3</sup>

Attempts to heat ferrous phosphate to temperatures above 900° in sealed evacuated quartz tubes resulted in the quartz being attacked. Therefore, crystals were grown by sintering in the following manner. Fe<sub>3</sub>(PO<sub>4</sub>)<sub>2</sub> was packed into a gold tube (5 mm in diameter, 40 mm long) which had been welded shut at one end. This open capsule was then sealed under vacuum in a quartz tube and heated for 3 days at 1025°. Crystals up to a few tenths of 1 mm in size could be picked out of the sintered mass.

**X-Ray Diffraction Data.** A powder diffraction pattern was taken of a sample of ground single crystals on a Norelco diffractometer equipped with a graphite monochromator at a scan speed of  $1/2^\circ$   $2\theta$ /min using Cu K $\alpha$  radiation. Table II presents the results of a least-squares refinement of these data indexed on the basis of a monoclinic unit cell.

A suitable crystal was ground to a sphere of radius 0.055 mm. Precession photographs revealed monoclinic symmetry with systematic absences confirming the space group  $P2_1/c$ .

The lattice parameters were determined in a PICK II least-squares

refinement program using 48 reflections within the angular range  $35^\circ < 2\theta < 47^\circ$ ; the reflections were automatically centered on a Picker FACS-I four-circle diffractometer using Mo K $\alpha_1$  radiation. At  $2\theta^\circ$  the lattice parameters are  $a = 8.881$  (2) Å,  $b = 11.169$  (2) Å,  $c = 6.145$  (1) Å, and  $\beta = 99.36$  (3)°, where the figures in parentheses represent the standard deviations in the last reported figure. The calculated density, with  $Z = 4$ , is 3.948 g/cm<sup>3</sup>.

Diffraction intensities were measured using Zr-filtered Mo K $\alpha$  radiation at a takeoff angle of 2.5° with the diffractometer operating in the  $\theta$ - $2\theta$  scan mode. Scans were made at 1°/min over 1.5° with allowance for dispersion and with 40-sec background counts taken at both ends of the scan. Of the 2150 independent data investigated in the angular range  $2\theta < 65^\circ$ , 1766 were considered observable according to the criterion  $|F_o| > 0.8\sigma_F$ , where  $\sigma_F$  is defined as  $0.02|F_o| + [C + k^2B]^{1/2}/2|F_o|Lp$ ; the total scan count is  $C$ ,  $k$  is the ratio of scanning time to the total background time, and  $B$  is the total background count. Three reflections were systematically monitored and no random variations in intensity greater than 3% were observed over the data collection period; the mean variation was very much smaller.

The intensity data were corrected for Lorentz and polarization effects and absorption corrections<sup>4</sup> were applied for a spherical crystal with  $\mu_R = 0.43$ ; the maximum absorption correction applied was 5.0% of  $|F_o|$ .

**Determination and Refinement of the Structure.** The atomic positional parameters reported for graftonite<sup>2</sup> were used as the initial trial structure. Four cycles of least-squares refinement<sup>5</sup> of these positions using a  $1/\sigma^2$  weighting scheme, zerovalent scattering factors for Fe, P and O,<sup>6</sup> isotropic temperature factors, and corrections for secondary extinction and anomalous dispersion yielded a residual  $R = 0.092$  ( $R_w = 0.121$ ). The anisotropic refinement, based on a data to parameter ratio of 15:1 with 119 independently varied parameters, converged to a final  $R = 0.048$  ( $R_w = 0.066$ ) for the observed data. In the final refinement, the maximum extinction correction<sup>7</sup> was 3% of  $|F_o|$  for the 10 $\bar{2}$  reflection.

Table III presents the final anisotropic coordinates and anisotropic thermal parameters.

(4) "International Tables for X-Ray Crystallography," Vol. II, Kynoch Press, Birmingham, England, 1968, p 295.

(5) W. R. Busing, K. O. Martin, and H. A. Levy, ORFLS, Report ORNL-TM-305, Oak Ridge National Laboratory, Oak Ridge, Tenn., 1962.

(6) D. T. Cromer and J. B. Mann, *Acta Crystallogr., Sect. A*, **24**, 321 (1968).

(7) W. H. Zachariasen, *Acta Crystallogr.*, **23**, 558 (1967); *Acta Crystallogr., Sect. A*, **24**, 324 (1968).

(1) M. L. Lindberg, *Amer. Mineral.*, **35**, 59 (1950).

(2) C. Calvo, *Amer. Mineral.*, **53**, 742 (1968).

(3) J. Korinth and P. Royen, *Z. Anorg. Allg. Chem.*, **313**, 121 (1961).

Table I. Compounds with the Graftonite Structure<sup>a</sup>

	<i>a</i> , Å	<i>b</i> , Å	<i>c</i> , Å	$\beta$ , deg	<i>V</i> , Å <sup>3</sup>	Cation CN	Ref
Fe <sub>3</sub> (PO <sub>4</sub> ) <sub>2</sub>	8.881 (2)	11.169 (2)	6.145 (1)	99.36 (3)	601	6:5:5	<i>b</i>
Graftonite	8.91 (1)	11.58 (1)	6.239 (8)	98.9 (1)	636	7:5:5	<i>d</i>
Mn <sub>3</sub> (PO <sub>4</sub> ) <sub>2</sub>	8.80 (1)	11.45 (2)	6.25 (5)	98.3 (2)	623	<i>c</i>	<i>e</i>
CdZn <sub>2</sub> (PO <sub>4</sub> ) <sub>2</sub>	9.032 (4)	11.417 (5)	5.952 (6)	98.8 (2)	607	7:4:5	<i>f</i>
Cd <sub>2</sub> Zn(PO <sub>4</sub> ) <sub>2</sub>	9.056 (8)	11.86 (1)	6.190 (9)	100.1 (2)	655	7:5:5	<i>f</i>
Cd <sub>3</sub> (AsO <sub>4</sub> ) <sub>2</sub>	9.285 (1)	11.936 (1)	6.599 (1)	98.45 (2)	723	6:5:5	<i>g</i>

<sup>a</sup> Figures in parentheses are esd's in the last reported figures. <sup>b</sup> This work. <sup>c</sup> No structure determination made. <sup>d</sup> Reference 2. <sup>e</sup> J. S. Stephens, Ph.D. Thesis, McMaster University, 1967. <sup>f</sup> C. Calvo and J. S. Stephens, *Can. J. Chem.*, **46**, 903 (1968). <sup>g</sup> G. Engel and W. Klee, *Z. Kristallogr., Kristallgeometrie, Kristallphys., Kristallchem.*, **132**, 332 (1970).

Table II. X-Ray Powder Diffraction Pattern of Fe<sub>3</sub>(PO<sub>4</sub>)<sub>2</sub><sup>a</sup>  
(*a* = 8.876 (2) Å, *b* = 11.162 (3) Å, *c* = 6.143 (2) Å,  $\beta$  = 99° 21 (2)')

<i>h k l</i>	<i>I</i>	<i>d</i> <sub>obsd</sub>	<i>d</i> <sub>calcd</sub>	<i>h k l</i>	<i>I</i>	<i>d</i> <sub>obsd</sub>	<i>d</i> <sub>calcd</sub>
1 1 1	8	4.286	4.287	-4 2 1	4	2.0281	2.0268
0 2 1	4	4.095	4.106	1 5 1	24	2.0107	2.0120
2 1 0	6	4.070	4.076	2 5 0	4	1.9901	1.9889
-2 1 1	16	3.664	3.648	-3 3 2	9	1.9548	1.9548
1 3 0	100	3.419	3.424	3 0 2	8	1.9445	1.9501
-2 2 1	13	3.166	3.175	-2 5 1	24	1.9328	1.9328
-1 3 1	4	3.062	3.066	-2 1 3	4	1.9293	1.9304
0 0 2	11	3.039	3.031	-4 0 2	21	1.9293	1.9299
-1 0 2	47	3.018	3.020	-4 1 2	3	1.9012	1.9018
0 1 2	12	2.942	2.925	3 4 1	8	1.8520	1.8526
3 0 0	11	2.936	2.919	-2 2 3	11	1.8492	1.8492
-1 1 2	49	2.915	2.915	1 2 3	4	1.8004	1.8005
1 3 1	40	2.906	2.904	-1 5 2	9	1.7951	1.7952
2 2 1	74	2.839	2.843	-1 3 3	11	1.7901	1.7908
2 3 0	71	2.834	2.835	0 6 1	17	1.7784	1.7785
0 4 0	28	2.788	2.790	-1 6 1	2	1.7596	1.7594
-3 1 1	54	2.726	2.730	5 0 0	6	1.7502	1.7515
-2 0 2	7	2.704	2.706	-5 1 1	4	1.7390	1.7393
-1 2 2	17	2.656	2.656	4 3 1	9	1.7335	1.7340
1 4 0			2.659	5 1 0	10	1.7305	1.7304
1 1 2	19	2.652	2.652	3 3 2	10	1.7278	1.7272
-3 2 1	7	2.5149	2.5135	-2 5 2	10	1.7229	1.7222
-1 4 1	5	2.4816	2.4803	-4 4 1	13	1.7166	1.7156
-2 2 2	8	2.4376	2.4353	2 1 3	19	1.7101	1.7103
3 1 1	19	2.4168	2.4185	5 2 0	2	1.6720	1.6712
1 4 1	4	2.3901	2.3919	3 5 1	8	1.6587	1.6584
0 3 2	9	2.3480	2.3498	0 4 3	6	1.6385	1.6366
-3 0 2	14	2.2956	2.2975	4 1 2	7	1.6369	1.6341
3 3 0			2.2967	2 5 2	7	1.6089	1.6092
-2 4 1	12	2.2596	2.2615	-4 1 3	19	1.6050	1.6052
-3 3 1	6	2.2450	2.2450	0 6 2			1.5855
1 3 2	3	2.1999	2.2012	5 3 0	4	1.5858	1.5847
4 0 0	4	2.1882	2.1894	1 7 0	13	1.5692	1.5688
4 1 0	6	2.1479	2.1485	5 2 1	2	1.5502	1.5506
2 2 2	5	2.1415	2.1436	-1 0 4	3	1.5349	1.5358
-3 2 2	3	2.1238	2.1245	0 0 4	12	1.5154	1.5154
-1 4 2	2	2.0522	2.0495	3 6 1	12	1.4879	1.4876
4 2 0	2	2.0382	2.0382				

<sup>a</sup> Powder diffractometer data; Cu K $\alpha$  radiation.

## Results and Discussion

Ferrous phosphate is isotypic with graftonite. The two isolated phosphate tetrahedra are fairly regular with average bond lengths of 1.534 Å (+0.007, -0.016 Å) for P(1) and 1.535 Å (+0.009, -0.016 Å) for P(2) and an average bond angle of 109.3° [+5.4, -4.8° for P(1); +3.1, -6.9° for P(2)]. Table IV lists the tetrahedral bond angles and distances. The standard deviations for all bond lengths and angles were computed by the function and error program ORFFE.<sup>8</sup>

Table V lists the bond distances and angles for the three distinct iron polyhedra. Fe(2) and Fe(3) are irregularly coordinated by five oxygen atoms while Fe(1) has six nearest oxygen atoms in the shape of a highly distorted octahedron.

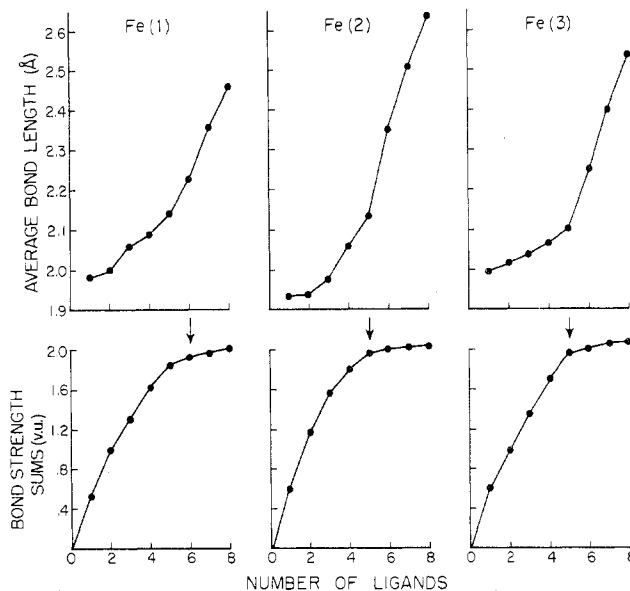


Figure 1. Average Fe-O bond lengths and bond strength sums around Fe vs. the number of coordinating ligands.

Although there is no problem in defining the primary coordination spheres of Fe(2) and Fe(3), there is an ambiguity in whether to assign O(7) at the fairly long distance of 2.682 Å to the primary coordination sphere of Fe(1). The M(1) site in graftonite is seven-coordinated in the form of a pentagonal bipyramid.<sup>2</sup> The Fe(1) site in Fe<sub>3</sub>(PO<sub>4</sub>)<sub>2</sub> is generated by removing the seventh oxygen [an O(3) at 2.69 Å in graftonite] from the pentagonal basal plane to a distance of 3.12 Å in Fe<sub>3</sub>(PO<sub>4</sub>)<sub>2</sub>. The second longest M(1)-O bond in graftonite is to O(7) at 2.58 Å which is the oxygen in question in Fe<sub>3</sub>(PO<sub>4</sub>)<sub>2</sub>.

As a help in justifying our choice to include O(7) in the coordination sphere of Fe(1), we have calculated the individual bond strengths (in valence units) using the formula given by Brown and Shannon:<sup>9</sup>  $s = s_0(R/R_0)^{-N}$ , where *s* is the strength (in valence units) of a bond of length *R*, *s*<sub>0</sub> is the ideal strength of the bond of length *R*<sub>0</sub>, and *N* is a characteristic constant. Values for *s*<sub>0</sub>, *R*<sub>0</sub>, and *N* for divalent iron are taken from the empirically fit values of ref 9 as 0.333, 2.155, and 5.5, respectively. Figure 1 illustrates plots of average bond lengths and bond strength sums vs. the number of coordinating ligands for each of the three iron sites. The bond strength sum plot should level off at  $\Sigma s = z$  (the valence of the ion).<sup>9</sup> A coordination number of 5 for Fe(1) gives a bond strength sum of 1.84; going to coordination number 6 raises it to 1.95. Note that a coordination number of 5 for Fe(2) and Fe(3) gives bond strength sums of 1.98 and 1.97, respectively. Using six-coordination for Fe(1) gives

(8) W. R. Busing, K. O. Martin, and H. A. Levy, ORFFE, Report ORNL-TM-306, Oak Ridge National Laboratory, Oak Ridge, Tenn., 1962.

(9) I. D. Brown and R. D. Shannon, *Acta Crystallogr., Sect. A*, **29**, 266 (1973).

Table III. Fractional Atomic Coordinates and Anisotropic Thermal Parameters<sup>a</sup>

Atom	10 <sup>4</sup> x	10 <sup>4</sup> y	10 <sup>4</sup> z	$\beta_{11}$	$\beta_{22}$	$\beta_{33}$	$\beta_{12}$	$\beta_{13}$	$\beta_{23}$
Fe(1)	9298 (1)	1159 (1)	8685 (1)	0.91 (3)	0.43 (3)	1.11 (3)	-0.13 (2)	-0.23 (2)	0.03 (2)
Fe(2)	7230 (1)	810 (1)	3307 (1)	1.56 (4)	1.75 (4)	0.40 (3)	0.86 (3)	0.19 (2)	0.11 (2)
Fe(3)	3630 (1)	1935 (1)	1188 (1)	0.56 (3)	0.60 (3)	0.57 (3)	0.09 (2)	0.01 (2)	-0.02 (2)
P(1)	942 (1)	1360 (1)	3911 (2)	0.43 (4)	0.26 (4)	0.46 (4)	-0.03 (3)	0.01 (3)	0.03 (3)
P(2)	6046 (1)	876 (1)	8053 (2)	0.46 (4)	0.48 (4)	0.32 (4)	0.05 (3)	0.07 (3)	0.08 (3)
O(1)	759 (4)	633 (3)	1750 (6)	0.64 (13)	0.83 (13)	0.61 (13)	0.13 (10)	-0.17 (10)	-0.30 (10)
O(2)	4810 (5)	1789 (4)	8262 (6)	0.96 (14)	1.10 (14)	0.54 (13)	0.55 (11)	0.28 (10)	0.13 (10)
O(3)	9472 (4)	2075 (4)	3940 (7)	0.43 (12)	0.93 (14)	1.13 (14)	0.44 (10)	0.17 (10)	-0.04 (11)
O(4)	6984 (4)	1259 (4)	6275 (6)	0.61 (13)	1.17 (14)	0.44 (12)	-0.01 (10)	0.29 (10)	0.10 (10)
O(5)	2274 (5)	2225 (4)	3752 (6)	0.91 (14)	1.09 (14)	0.69 (13)	-0.40 (11)	0.32 (11)	-0.18 (11)
O(6)	7250 (4)	866 (4)	153 (6)	0.46 (12)	1.09 (14)	0.78 (13)	0.14 (10)	-0.04 (10)	0.04 (11)
O(7)	1296 (4)	616 (3)	5999 (6)	0.72 (13)	0.60 (13)	0.79 (13)	0.12 (10)	-0.17 (11)	0.16 (10)
O(8)	5338 (5)	-382 (3)	7617 (7)	1.14 (15)	0.45 (13)	0.88 (14)	0.05 (11)	0.01 (11)	0.03 (10)

<sup>a</sup> Numbers in parentheses are estimated standard deviations in the last significant figure.

Table IV. Bond Distances, Polyhedral Edge Lengths, and Bond Angles for the Phosphate Tetrahedra<sup>a</sup>

(i) Interatomic Distances, Å			
P(1)-O(1)	1.543 (4)	P(2)-O(2)	1.519 (4)
P(1)-O(3)	1.532 (4)	P(2)-O(4)	1.539 (4)
P(1)-O(5)	1.543 (4)	P(2)-O(6)	1.536 (4)
P(1)-O(7)	1.518 (4)	P(2)-O(8)	1.544 (4)

P(1) Tetrahedron		P(2) Tetrahedron	
O(1)-O(3)	2.493 (5)	O(2)-O(4)	2.517 (5)
O(1)-O(5)	2.440 (6)	O(2)-O(6)	2.508 (6)
O(1)-O(7)	2.577 (6)	O(2)-O(8)	2.513 (6)
O(3)-O(5)	2.516 (6)	O(4)-O(6)	2.397 (5)
O(3)-O(7)	2.492 (5)	O(4)-O(8)	2.562 (6)
O(5)-O(7)	2.506 (6)	O(6)-O(8)	2.528 (6)

## (ii) Angles, Deg

P(1) Tetrahedron		P(2) Tetrahedron	
O(1)-P(1)-O(3)	108.3 (2)	O(2)-P(2)-O(4)	110.8 (2)
O(1)-P(1)-O(5)	104.5 (2)	O(2)-P(2)-O(6)	110.4 (2)
O(1)-P(1)-O(7)	114.7 (2)	O(2)-P(2)-O(8)	110.3 (2)
O(3)-P(1)-O(5)	109.8 (2)	O(4)-P(2)-O(6)	102.4 (2)
O(3)-P(1)-O(7)	109.5 (2)	O(4)-P(2)-O(8)	112.4 (2)
O(5)-P(1)-O(7)	109.9 (2)	O(6)-P(2)-O(8)	110.3 (2)

<sup>a</sup> Numbers in parentheses are estimated standard deviations in the last significant figure.

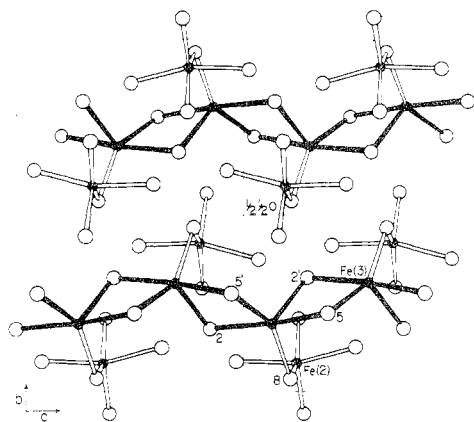


Figure 2. Projection of the  $\text{Fe}_3(\text{PO}_4)_2$  structure onto the  $bc$  plane. The chains of edge-sharing  $\text{Fe}(3)$  polyhedra are outlined.

an average  $\text{Fe}^{2+}$ -oxygen distance of 2.23 Å as compared to an average distance of 2.13 and 2.10 Å for five-coordinated  $\text{Fe}(2)$  and  $\text{Fe}(3)$ , respectively, and a calculated value of 2.15 Å for six-coordinated  $\text{Fe}^{2+}$  using Shannon and Prewitt's ionic radii.<sup>10</sup> [It should be noted, however, that five-coordination about  $\text{Fe}(1)$  gives an average bond distance of 2.14 Å.] This assignment of coordination (6:5:5) results in

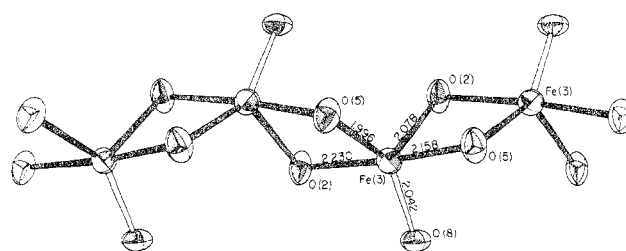


Figure 3. View (onto the  $bc$  plane) of a chain of  $\text{Fe}(3)$  polyhedra. Thermal ellipsoids of vibration (98%) are shown.

each oxygen atom being bonded to one phosphorus and two iron atoms.

Figure 2 is a projection of a part of the structure of  $\text{Fe}_3(\text{PO}_4)_2$  onto the  $bc$  plane (centered about  $1/2, 1/2, 0$ ) and illustrates the chains of edge-sharing  $\text{Fe}(3)$  polyhedra which are a building block of both the ferrous phosphate and graftonite structures. These chains, linked through  $\text{O}(2)$  and  $\text{O}(5)$ , lie parallel to the  $c$  axis and are further joined to isolated  $\text{Fe}(2)$  polyhedra through  $\text{O}(8)$ . [All of the crystallographic drawings were made using a local modification of the program ORTEP.<sup>11</sup>] Figure 3 is a similar view of the chain of edge-sharing  $\text{Fe}(3)$  polyhedra including thermal ellipsoids of vibration (98%).

Figure 4 is a projection of another part of the structure onto the  $ab$  plane centered about  $1/2, 1/2, 0$  illustrating the  $\text{Fe}(1)$  "dimers" which are centered about the crystallographic center of symmetry. These dimers share an edge formed by  $\text{O}(1)$  and  $\text{O}(1')$  and corner-link through the four other oxygen atoms attached to each  $\text{Fe}(1)$  to four  $\text{Fe}(2)$  atoms (only one  $\text{Fe}(2)$ , linked through  $\text{O}(3)$ , is shown in the figure). The  $\text{Fe}(3)$  chains run into the plane of the figure at the monoclinic angle. In graftonite, these dimeric  $\text{Fe}(1)$  units are directly connected through a corner formed by an additional  $\text{O}(3)$  atom (which gives each  $\text{M}(1)$  site seven-coordination); this results in a net of  $\text{Fe}(1)$  polyhedra parallel to the  $bc$  plane.

A closer view of the  $\text{Fe}(1)$  dimer is given in Figure 5 which includes thermal ellipsoids (98%). As in Figure 4, the  $b$  axis is vertical, but the  $a$  axis has been rotated  $\sim 35^\circ$  into the plane of the drawing for greater clarity. The  $\text{Fe}(1)$ - $\text{Fe}(1)$  distance is 3.195 Å which, although not unusually short, is substantially less than the 3.51 Å observed in graftonite (the next shortest iron-iron distance in  $\text{Fe}_3(\text{PO}_4)_2$  is  $\text{Fe}(3)$ - $\text{Fe}(3)$  at 3.32 Å which is comparable to 3.40 Å in graftonite).

As Calvo and Stephens have pointed out,<sup>12</sup> the graftonite

(10) R. D. Shannon and C. T. Prewitt, *Acta Crystallogr., Sect. B*, 25, 925 (1969).

(11) C. K. Johnson, ORTEP, Report ORNL-3794, Oak Ridge National Laboratory, Oak Ridge, Tenn., 1965.

(12) C. Calvo and J. S. Stephens, *Can. J. Chem.*, 46, 903 (1968).

Table V. Bond Distances, Polyhedral Edge Lengths, and Bond Angles for the Iron Polyhedra<sup>a</sup>

(i) Interatomic Distances, Å					
Fe(1)-O(3)	1.983 (4)	Fe(2)-O(4)	1.938 (4)	Fe(3)-O(5')	1.996 (4)
Fe(1)-O(1')	2.018 (4)	Fe(2)-O(6)	1.942 (4)	Fe(3)-O(8)	2.042 (4)
Fe(1)-O(6)	2.182 (4)	Fe(2)-O(7)	2.062 (4)	Fe(3)-O(2')	2.078 (4)
Fe(1)-O(1)	2.186 (4)	Fe(2)-O(8)	2.309 (5)	Fe(3)-O(5)	2.158 (4)
Fe(1)-O(4)	2.332 (4)	Fe(2)-O(3)	2.420 (4)	Fe(3)-O(2)	2.230 (4)
Fe(1)-O(7)	2.682 (4)				

Fe(1) Polyhedron <sup>b</sup>		Fe(2) Polyhedron		Fe(3) Polyhedron	
O(1)-O(1')	2.737 (8)	O(3)-O(4)	2.967 (6)	O(2)-O(2')	3.458 (4)
O(1)-O(3)	3.144 (6)	O(3)-O(6)	3.105 (6)	O(2)-O(5)	4.378 (6)
O(1)-O(6)	3.122 (6)	O(3)-O(7)	3.083 (6)	O(2)-O(5')	2.568 (6)
O(1)-O(7)	3.642 (6)	O(3)-O(5)	4.627 (6)	O(2)-O(8)	3.002 (6)
O(1')-O(4)	3.027 (5)	O(4)-O(6)	3.833 (6)	O(2')-O(5)	2.568 (6)
O(1')-O(6)	2.823 (6)	O(4)-O(7)	3.060 (6)	O(2')-O(5')	3.310 (6)
O(1')-O(7)	2.831 (6)	O(4)-O(8)	3.054 (6)	O(2')-O(8)	3.204 (6)
O(3)-O(4)	3.139 (6)	O(6)-O(7)	3.001 (5)	O(5)-O(5')	3.133 (2)
O(3)-O(6)	3.197 (6)	O(6)-O(8)	2.911 (6)	O(5)-O(8)	3.166 (6)
O(3)-O(7)	3.674 (6)	O(7)-O(8)	3.736 (6)	O(5')-O(8)	3.883 (6)
O(4)-O(6)	2.397 (5)				
O(4)-O(7)	3.427 (6)				

(ii) Angles, Deg					
Fe(1) Polyhedron		Fe(2) Polyhedron		Fe(3) Polyhedron	
O(1)-Fe(1)-O(1')	81.1 (2)	O(3)-Fe(2)-O(4)	85.0 (2)	O(2)-Fe(3)-O(2')	106.7 (2)
O(1)-Fe(1)-O(3)	99.9 (2)	O(3)-Fe(2)-O(6)	90.1 (2)	O(2)-Fe(3)-O(5)	172.5 (2)
O(1)-Fe(1)-O(6)	91.3 (1)	O(3)-Fe(2)-O(7)	86.5 (1)	O(2)-Fe(3)-O(5')	74.6 (2)
O(1)-Fe(1)-O(7)	96.3 (1)	O(3)-Fe(2)-O(8)	156.1 (1)	O(2)-Fe(3)-O(8)	89.1 (2)
O(1')-Fe(1)-O(4)	87.9 (1)	O(4)-Fe(2)-O(6)	162.2 (2)	O(2')-Fe(3)-O(5)	74.6 (1)
O(1')-Fe(1)-O(6)	84.4 (2)	O(4)-Fe(2)-O(7)	99.8 (2)	O(2')-Fe(3)-O(5')	108.7 (2)
O(1')-Fe(1)-O(7)	72.5 (1)	O(4)-Fe(2)-O(8)	91.5 (2)	O(2')-Fe(3)-O(8)	102.1 (1)
O(3)-Fe(1)-O(4)	93.0 (2)	O(6)-Fe(2)-O(7)	97.1 (2)	O(5)-Fe(3)-O(5')	97.9 (2)
O(3)-Fe(1)-O(6)	100.1 (2)	O(6)-Fe(2)-O(8)	86.0 (2)	O(5)-Fe(3)-O(8)	97.8 (2)
O(3)-Fe(1)-O(7)	102.8 (1)	O(7)-Fe(2)-O(8)	117.3 (2)	O(5')-Fe(3)-O(8)	148.2 (2)
O(4)-Fe(1)-O(6)	64.0 (1)				
O(4)-Fe(1)-O(7)	102.9 (1)				
O(1)-Fe(1)-O(4)	153.9 (1)				
O(1')-Fe(1)-O(3)	175.4 (3)				
O(6)-Fe(1)-O(7)	154.1 (1)				

<sup>a</sup> Numbers in parentheses are estimated standard deviations in the last significant figure. <sup>b</sup> Octahedral edges only.

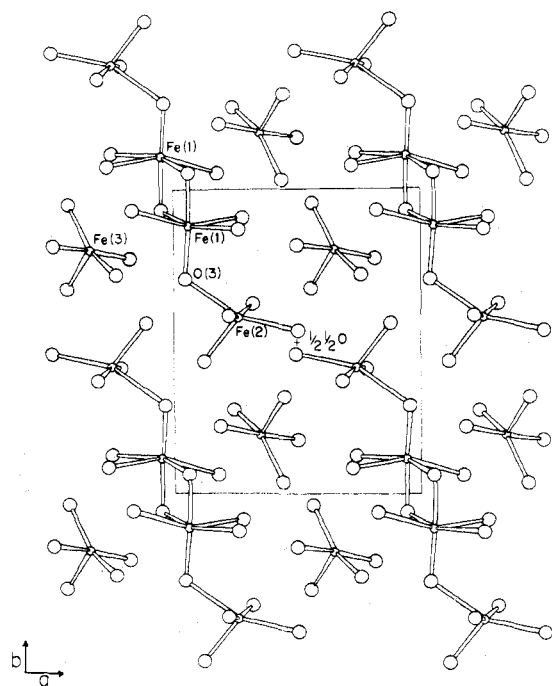


Figure 4. Projection of the  $\text{Fe}_3(\text{PO}_4)_2$  structure onto the  $ab$  plane.

structure is unusual in its ability, through small changes in atomic positions, to vary the cation coordination numbers while maintaining the basic structure type. Reference to Table I illustrates the variety of cation coordination num-

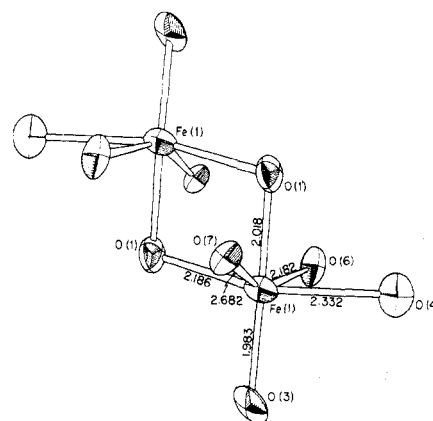


Figure 5. View of the Fe(1) dimer including thermal ellipsoids of vibration (98%). The  $b$  axis is vertical (as in Figure 4), but the  $a$  axis is rotated  $\sim 35^\circ$  into the plane of the drawing for clarity.

bers found among these compounds. While the coordination number of the M(3) position remains at 5, the shift from five- to four-coordination for the M(2) site in going from  $\text{Cd}_2\text{Zn}(\text{PO}_4)_2$  to  $\text{CdZn}_2(\text{PO}_4)_2$  is certainly a size effect.<sup>12</sup> Seven-coordination about the M(1) site in graftonite has been shown<sup>2</sup> to be associated with the preference of the large  $\text{Ca}^{2+}$  ion for this site. This seven-coordination persists for the similar  $\text{Cd}^{2+}$  ion in  $\text{Cd}_2\text{Zn}(\text{PO}_4)_2$  and  $\text{CdZn}_2(\text{PO}_4)_2$ .<sup>12</sup> However, in  $\text{Cd}_3(\text{AsO}_4)_2$  the M(1) site is six-coordinated.<sup>13</sup>

(13) G. Engel and W. Klee, *Z. Kristallogr., Kristallgeometrie, Kristallphys., Kristallchem.*, 132, 332 (1970).

Perhaps this is due to the larger  $\text{AsO}_4^{3-}$  ion relative to  $\text{PO}_4^{3-}$ ; note the substantial increase in cell volume (Table I). Obviously, it is the smaller ferrous ion ( $r = 0.75 \text{ \AA}$ ) that allows the collapse of the seven-coordinated M(1) site in graftonite to six-coordination in  $\text{Fe}_3(\text{PO}_4)_2$ . The additional stability gained by a possible Fe(1)-Fe(1) interaction (indicated by the shorter bond distance) may also contribute to the lower coordination. [Our Mossbauer measurements of  $\text{Fe}_3(\text{PO}_4)_2$  at  $77^\circ\text{K}$  do not show the presence of magnetic order.] It would be of interest to complete a detailed structural analysis of  $\text{Mn}_3(\text{PO}_4)_2$  in order to elaborate upon this analysis.

**Acknowledgments.** This work was supported by the University of Connecticut Research Foundation. Computa-

tions were carried out in the Computer Center of the University of Connecticut.

Registry No.  $\text{Fe}_3(\text{PO}_4)_2$ , 14940-41-1.

**Supplementary Material Available.** A listing of calculated and observed structure factors will appear following these pages in the microfilm edition of this volume of the journal. Photocopies of the supplementary material from this paper only or microfiche (105 × 148 mm, 24X reduction, negatives) containing all of the supplementary material for the papers in this issue may be obtained from the Journals Department, American Chemical Society, 1155 16th Street, N.W., Washington, D. C. 20036. Remit check or money order for \$3.00 for photocopy or \$2.00 for microfiche, referring to code number INORG-74-2876.

Contribution from the Chemistry Department, Ohio University, Athens, Ohio 45701, and University of Houston, Houston, Texas 77004

## Structural Studies of $(\pi\text{-C}_5\text{H}_5)_2\text{MX}_2$ Complexes and Their Derivatives. Structure of (1,1'-Trimethylene- $\pi$ -dicyclopentadienyl)hafnium Dichloride

CARLOS H. SALDARRIAGA-MOLINA,<sup>1</sup> A. CLEARFIELD,\* and IVAN BERNAL

Received July 5, 1974

AIC40442Y

(1,1'-Trimethylene- $\pi$ -dicyclopentadiene)hafnium dichloride,  $(\text{CH}_2)_3(\text{C}_5\text{H}_4)_2\text{HfCl}_2$ , is orthorhombic, space group *Pbca*, and isomorphous with the corresponding zirconium compound. The unit cell dimensions are  $a = 8.177$  (3)  $\text{\AA}$ ,  $b = 13.916$  (4)  $\text{\AA}$ , and  $c = 22.425$  (9)  $\text{\AA}$ , with  $Z = 8$ . The structure was determined from three-dimensional X-ray data (1797 independent reflections), obtained by means of an automated four-circle diffractometer, and refined anisotropically to an  $R$  of 0.029. The coordination about the hafnium atom is that of a distorted tetrahedron comprised of the chlorine atoms and the centroids of the  $\pi$ -cyclopentadienyl rings. The Cl-Hf-Cl bond angle is  $95.87$  (8) $^\circ$  and the centroid-Hf-centroid angle  $129.5^\circ$ . The Hf-Cl bond distances are 2.417 (3) and 2.429 (2)  $\text{\AA}$ . These are slightly smaller than the corresponding bond distances in the zirconium complex and are in agreement with the sum of the Pauling radii. Distances from the hafnium atom to the ring centroids are 2.170 and 2.181  $\text{\AA}$  and the range of Hf-C distances is 2.459-2.501  $\text{\AA}$ . The carbon-carbon bond distances within the cyclopentadiene rings average 1.404  $\text{\AA}$  and range from 1.368 (17) to 1.438 (12)  $\text{\AA}$ . These parameters not only establish the pentahapto nature of the metal-ring bonding but indicate that when the thermal motion of the rings is reduced by the constraints of the exocyclic bridge, the C-C bond lengths have a narrower range and calculate closer to the expected value of 1.41  $\text{\AA}$ .

### Introduction

This study is a continuation of our research into the chemistry and stereochemistry of dicyclopentadienyl compounds of the group IVb transition elements. The study of the title substance was prompted by the following considerations.

(a) Previous studies by Davis and Bernal<sup>2,3</sup> and by Epstein and Bernal<sup>4</sup> have shown that the C-C bond lengths of the  $\pi$ -cyclopentadiene rings vary according to the degree of librational motion about the metal-ring centroid vector. In order to document this observation with additional data, we have undertaken a study of the series of compounds with formulas  $(\pi\text{-C}_5\text{H}_5)_2\text{MCl}_2$  and  $(\text{CH}_2)_3(\pi\text{-C}_5\text{H}_4)_2\text{MCl}_2$ , where  $\text{M} = \text{Ti, Zr, Hf}$ . The object of the comparison is to demonstrate that in the latter series of compounds, where thermal motion is severely hindered by the aliphatic chain linking the  $\pi\text{-C}_5\text{H}_4$  moieties, the C-C distances are more uniform. Inas-

much as there are no further changes in the two series, the conclusion that thermal motion is responsible for the large variations in C-C distances in the unbridged series would be unassailable, if experimentally substantiated by the structural results. The structure of  $(\text{CH}_2)_3(\pi\text{-C}_5\text{H}_4)_2\text{TiCl}_2$  has already been determined by X-ray<sup>2</sup> and by neutron diffraction<sup>4b</sup> methods. The structure of  $(\pi\text{-C}_5\text{H}_5)_2\text{TiCl}_2$  has been reported;<sup>5</sup> however, the refinement was apparently not carried to completion. We are currently redoing the X-ray structural analysis on an untwinned crystal of that substance.<sup>6</sup>

(b) Accurate studies of series of compounds like the group IVb cyclopentadienes and of homologous series of substances with larger and larger numbers of electrons in the d shells will be useful in deciding whether the so-called Ballhausen-Dahl<sup>7</sup> theory, the Alcock theory,<sup>8</sup> or some compromise between the two is the correct interpretation of the bonding in organometallics of the type  $(\pi\text{-C}_5\text{H}_5)_2\text{MX}_2$ .

(c) Finally, we were interested in establishing the effect of purity on the structural determination of hafnium com-

\* To whom correspondence should be addressed at Ohio University.

(1) This paper is one of a series based upon the Ph.D. thesis of C. H. S. presented to the Department of Chemistry, Ohio University, March 1974.

(2) B. R. Davis and I. Bernal, *J. Organometal. Chem.*, **30**, 75 (1971).

(3) B. R. Davis and I. Bernal, *J. Cryst. Mol. Struct.*, **2**, 135 (1972).

(4) (a) E. F. Epstein, I. Bernal, and H. Kopf, *J. Organometal. Chem.*, **26**, 229 (1971); (b) E. F. Epstein and I. Bernal, *Inorg. Chim. Acta*, **7**, 211 (1973).

(5) V. V. Tkachev and L. O. Otovmyan, *J. Struct. Chem. (USSR)*, **13**, 263 (1972).

(6) A. Clearfield, C. H. Saldarriaga-Molina, D. Warner, and I. Bernal, work in progress.

(7) C. J. Ballhausen and J. P. Dahl, *Acta Chem. Scand.*, **15**, 1333 (1961).

(8) N. W. Alcock, *J. Chem. Soc. A*, 2001 (1967).